Tailored functional monolayers made from mesoionic carbenes

Omar Sadek, Jad Rabah, Salem Ba Sowid, Dimitri Mercier, Philippe Marcus,
Clément Chauvier, François Ribot, Louis Fensterbank, Emmanuel
Maisonhaute

HAL Id: hal-04731857
https://hal.sorbonne-universite.fr/hal-04731857v2

Submitted on 11 Oct 2024
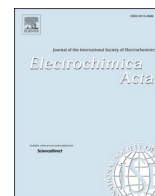
Tailored functional monolayers made from mesoionic carbenes

Omar Sadek [a,1], Jad Rabah [a,1], Salem Ba Sowid [a,b], Dimitri Mercier [c], Philippe Marcus [c], Clément Chauvier [a], François Ribot [a,*], Louis Fensterbank [a,d,*], Emmanuel Maisonhaute [a,*]

[a] Sorbonne Université, CNRS, Institut Parisien de Chimie Moléculaire (IPCM), 4 place Jussieu, CEDEX 05 F75252 Paris, France
[b] Sorbonne Université, CNRS, Laboratoire de Chimie de la Matière Condensée de Paris (LCMCP), 4 place Jussieu, CEDEX 05 75252 Paris, France
[c] PSL Research University, CNRS, Chimie ParisTech, Institut de Recherche de Chimie Paris (IRCP), Physical Chemistry of Surfaces Research Group, 11 rue Pierre et Marie Curie, 75005 Paris, France
[d] Collège de France, Chaire activation en chimie moléculaire, 11 place Marcelin Berthelot, 75005 Paris, France

A R T I C L E   I N F O

A B S T R A C T

Significant progress has been made over the last decades in surface functionalization of coinage metals using thiols and more recently N-heterocyclic carbenes. As shown in this work, mesoionic carbenes (MICs) provide straightforward access to a novel class of surface ligands including electroactive ones and thus materials. Importantly, MICs are easily accessed from triazolium salts (TS) onto which functional groups may be attached with little synthetic effort. Here, we present a library of TS that were further converted, *in situ*, into MICs and grafted onto gold surfaces. The modified surfaces were thoroughly characterized by advanced spectroscopic methods such as XPS, infrared and Tip-Enhanced Raman Spectroscopy. Through cyclic voltammetry at 100 Vs^{-1}, we could evaluate the surfacic concentration of the grafted molecules for electroactive MICs. We also prepared mixed MIC/thiol self-assembled monolayers, which opens the route to multifunctional surfaces.

1. Introduction

Tuning surface properties is crucial to many domains such as molecular electronics, (bio)sensing or energy harvesting, among others [1]. In the 1980s, the discovery of self-assembled monolayers (SAMs) provided a facile method for the attachment of thiol ligands to gold or silver surfaces allowing greater structural control compared to electropolymerization [2,3]. This discovery paved the way to a wealth of applications while also stimulating alternative surface modification strategies for the development of well-defined and robust interfaces on various substrates.

An alternative and interesting possibility is offered by grafting aryl diazonium or iodonium salts [4,5]. Here, aryl radicals, generated under negative potentials, illumination or spontaneously, may react and bind to the surface. However, controlling surface organization remains quite difficult despite the proposition of interesting yet elaborated strategies [6–8]. Often, these various protocols lead to non-homogeneous multilayers. Alternatively, hydrosilylation can be used to produce monolayers on silicon, but the approach is restricted to this substrate and requires rather harsh preparation conditions [9]. Hence, there is a demand for proposing novel, reproducible and robust synthetic routes towards SAMs.

For slightly more than a decade, (benz)imidazolium-based N-heterocyclic carbenes (NHCs), well-known ligands in organometallic chemistry, have appeared as promising surface anchors in material science [10–14]. Initially used to stabilize metallic nanoparticles [15–26], they were soon after studied on flat surfaces where they exhibit strong anchoring and simultaneously provide monolayers [27–33]. Some other types of carbenes have also been deposited on metallic surfaces: 1,2,4-triazolylidene [33], cyclic (alkyl)(amino)carbenes [34], cyclopropenylidenes [35], and very recently imidazo[1,2-a]pyridine [36]. However, a significant drawback of these NHCs emerges when non-symmetric, backbone-modified or functional analogues are required. Access is often difficult as it requires multiple synthetic steps or post-modification on a pre-functionalized surface which represents an equally complicated strategy [33,37]. As a consequence, this strategy remains rather underexploited in comparison to those cited above.

Herein, we describe an alternative approach with the potential of

---

solving the issues mentioned above. It relies on the use of 1,2,3-triazole-based mesoionic carbenes (MICs) as surface-capping ligands [38,39]. From a synthetic point of view, MICs are easily generated by deprotonation of their parent triazolium salts. These salts are readily obtained via the modular copper-catalyzed alkyne-azide cycloaddition (CuAAC) click reaction, followed by quaternization of the γ-nitrogen (N^3). This highlights a major advantage of MICs over NHCs in the simplicity of backbone modification through alkylation at the N^3 position. Moreover, the carbanionic character of the coordinating site makes MICs more σ-donating than classical Arduengo-type NHCs, *a priori* resulting in a stronger metal-carbene interaction when grafted on surfaces [36]. This has already been exploited for the synthesis of gold or silver nanoparticles[40–43] but, to the best of our knowledge, has never been described for surface functionalization prior our initial report [44].

Herein, we demonstrate that various easily-prepared MICs can be anchored to gold surfaces and provide careful characterization of the latter through X-ray photoelectron (XPS), infrared (IR) and Tip Enhanced Raman (TERS) spectroscopies. Electrochemical studies are also central to monitor monolayer formation and determine molecular coverages as a function of time. Finally, we also demonstrate that mixed MIC/thiol monolayers may be formed, opening an avenue to surfaces bearing different types of ligands, electroactive or not.

2. Synthesis and surface modification

At the outset of this study, we prepared the functionalized triazolium salts (**TS 1**–**5**) in two steps from the two common triazole precursors **6a-b** (Scheme 1a). Briefly, the latter heterocycles were readily obtained by a CuAAC click reaction and subsequently engaged in an alkylation step with an alkyl bromide (R^2–Br), some of them bearing specific functional groups such as a ferrocenyl moiety (**TS 1** and **TS 2**) or substituted arenes

(**TS 3** and **TS 4**). This pool of reagents not only allows us to investigate the generality of the gold surface functionalization event, but also conveys a specific purpose in that **TS 1**, **TS 2** and **TS 3** are electroactive and **TS 4** bears a biphenyl entity with a characteristic Raman spectroscopic signature. Triazolium **TS 5** was also studied as a reference to our former work on nanoparticles [43]. Detailed syntheses are provided in the Supporting Information (SI).

To assess the potential of the MICs derived from triazolium salts **TS 1**–**5** to functionalize gold surfaces or gold electrodes, we set out to prepare the free mesoionic carbenes **MIC 1**–**5** by deprotonation of **TS 1**–**5** prior to exposing them to a gold surface. To that end, we prepared 1 mM THF solutions of the triazolium precursors into which we added, under argon, 1 equivalent of *t*-BuONa as base (Scheme 2). Gold surfaces were subsequently introduced in the reactor and left in the carbene solution for times ranging from 5 min to 3 h. After thorough rinsing to remove any physisorbed molecules (see the SI for details), in-depth surface analytical methods were used to characterize the new materials and to assess the extent of surface coverage.

2.1. Spectroscopic investigations

Characterizations of gold surfaces functionalized with **MICs 1**–**5** were performed by XPS as shown in Fig. 1 (100 scans were collected to maximize the signal/noise ratio). As expected, peaks attributed to carbon (C1s $\sim$ 285 eV) and nitrogen (N1s $\sim$ 400 eV) are observed, in addition to those of gold, confirming the immobilization of the MIC on the surface (see Fig. S1). A fine analysis of the C1s and N1s peaks (presented in the SI) confirms the presence of the MIC. The N/C ratios are given in Table 1. The slightly lower N/C ratios observed can be explained by a stronger attenuation of the N signal, which comes from atoms screened by the alkyl chains, in agreement with an upright
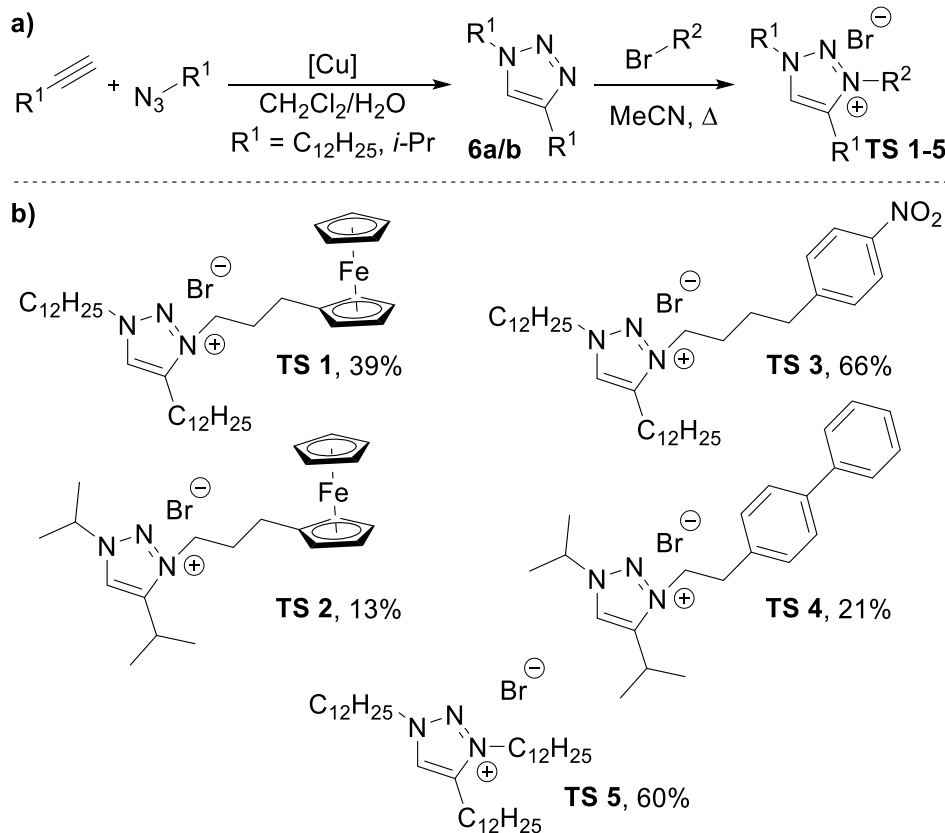
Scheme 1. (a) General synthetic route to functionalized triazolium salts **TS**. (b) Systems **TS 1**–**5** investigated in this study; yields are calculated over two synthetic steps.
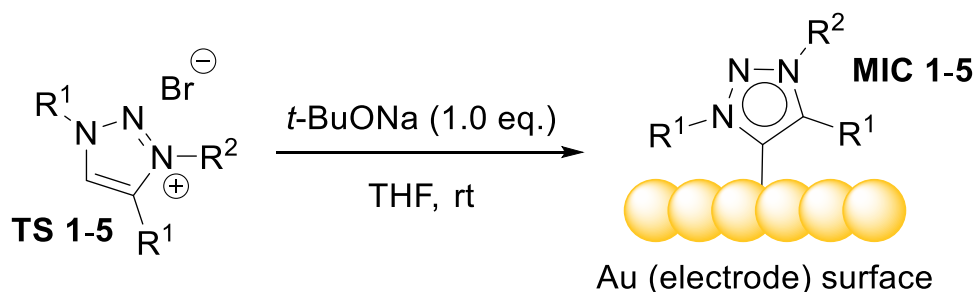
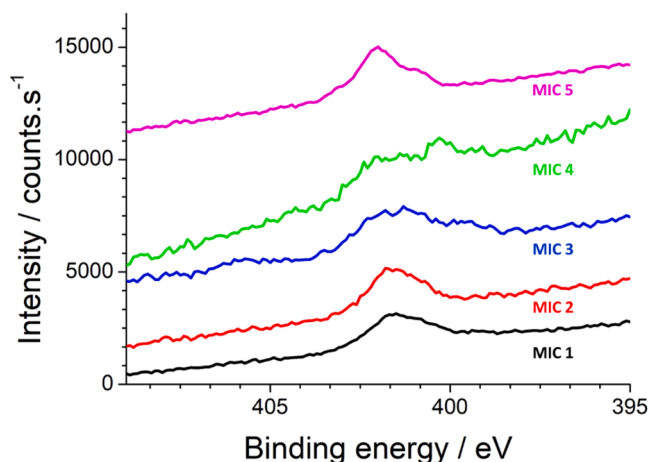**Scheme 2.** Gold surface or electrode functionalization with **MICs 1–5**.

Fig. 1. XPS spectra of N1s for **MICs 1–5** grafted on gold substrates.

Table 1

N/C ratio and surface coverage obtained for **MIC 1–5**. Theoretical N/C ratios are indicated in parenthesis.

MIC	N/C	Surface coverage
MIC 1	0.068 (0.076)	1.7×10^{-6} molm^{-2}
MIC 2	0.086 (0.14)	1.8×10^{-6} molm^{-2}
MIC 3	0.11 (0.11)	1.8×10^{-6} molm^{-2}
MIC 4	0.091 (0.14)	1.2×10^{-6} molm^{-2}
MIC 5	0.080 (0.078)	1.9×10^{-6} molm^{-2}

coordination geometry as depicted in Scheme 2.

The N1s peak can be split into two components at ~401.5 and ~400.0 eV with a 2:1 ratio corresponding to the different chemical environments of the nitrogen atoms [43]. Compared to the binding energy of the triazolium salt, a shift of 1.8 eV is observed toward lower binding energy. For **MIC 3** a third component at 405 eV, characteristic of the NO₂ group, is also observed. This shift already described previously on gold NPs confirms the covalent bond between the MIC and gold substrate [23,24,43]. We did not detect any Br, which indirectly confirms covalent grafting and the absence of physisorbed triazolium salt precursor. For each grafted MIC, a surface density has been estimated (see Table 1) by solving the set of equations given in the SI. The surface coverages are found within a range 1.2–1.9×10^{-6} molm^{-2} as expected for their similar structures.

Attenuated total reflectance (ATR) infrared measurements onto SAMs made from **MIC 1–3** and **MIC 5** on flat gold surfaces were also performed to verify that the molecular integrity of the surface ligands was preserved upon grafting. The recorded spectra and their analysis are provided in Figs. S2–5 and Table S1. All the assemblies showed characteristic bands corresponding to the specific pendant functional groups.

As an alternative spectroscopic approach, Surface Enhanced Raman Spectroscopy (SERS) has been formerly used to analyze the ligand shell around nanoparticles and assess their stability [45,46]. For our macroscopic surfaces, we resorted here to Tip Enhanced Raman Spectroscopy (TERS) that allows the observation, at the nanometer scale, of whether molecules are uniformly distributed or not. TERS advantageously combines scanning probe microscopy (here scanning tunneling microscopy) with SERS [47–55]. It requires the use of a tip for which the localized plasmon resonance can be stimulated using a laser of adapted wavelength so as to considerably amplify the electromagnetic field below the tip. In this study, we used a gold STM tip to image the surface and record Raman spectra for **MIC 4** adsorbed on a flat gold substrate over 180 min as presented in Fig. 2.

At each pixel acquired over a 100 ms integration time, we recorded a Raman spectrum, with a spatial resolution of a few nanometers as described in the SI. The average signal over the area is provided by the red trace in Fig. 2a. The characteristic features of the phenyl moieties' vibrations are apparent, with a clear similarity to 4-biphenylthiol signals, and in agreement with theoretical calculations reported in the SI (Table S2) [56,57]. This allowed us to construct the intensity map, presented in Fig. 2b, by integrating the phenyl rings breathing mode vibrations at 1609 cm⁻¹ over an area of 12×12 nm² (an average of four 6×6 nm² pixels in our acquisition procedure). The two other traces in Fig. 2a, corresponding to one rather intense (blue trace, red pixel in Fig. 2b) and one less intense (green trace, black pixel in Fig. 2b) pixel, show that in fact there is little intensity fluctuation. It is however difficult to ascertain if the observed variations are due to different local concentrations, orientation of the molecules or electromagnetic amplification. We emphasize that even at the dark pixel (green trace), the Raman spectrum still evidences the presence of **MIC4**. Overall, we can conclude that the whole surface was covered by **MIC 4**, with little concentration variations, and that there were no large areas without molecules. A TERS signal was also recorded with **MIC 3**, which presents an intense band at 1325 cm⁻¹ ascribed to the symmetric NO₂ stretching mode [58]. Spectroscopic and electrochemical data for this system are presented in Figs. S6–7.

2.2. Electroactive self-assembled monolayers

The spectroscopic evidences presented above confirm that MICs were efficiently grafted onto gold surfaces. In order to more accurately quantify the number of molecules present on the surface and assess the grafting kinetics, we used **MIC 2** that bears a redox tag. The molecular coverage was estimated by cyclic voltammetry (CV). In this approach, the number of redox entities grafted on an electrode as a function of immersion time could be easily followed by simple integration of the faradaic current peak. Indeed, when performing CV on a SAM, the faradaic charge that flows through the electrode is directly proportional to the number of adsorbed redox systems [59]. Experimentally, we resorted to gold balls that were flame annealed prior to immersion in **MIC 2** solutions for different times [60,61]. Their area was determined by CV in a reference ferrocene solution as described in SI. After rinsing, the electrodes were immersed in a 0.1 M tetrabutylammonium hexafluorophosphate solution (dichloromethane) as supporting electrolyte.
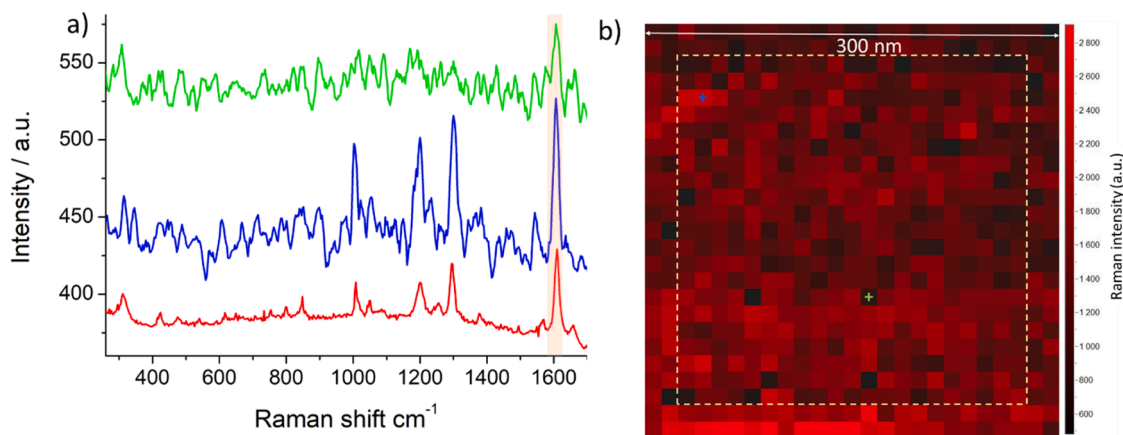
Fig. 2. (a) Average Raman spectrum of **MIC 4** (red). Spectra at a bright pixel (blue) and at a dark pixel (green) at positions indicated on (b). (b) TERS intensity map of **MIC4** obtained by integration of the band between 1582 and 1643 cm^{-1}, highlighted in pale red in Fig. 2a; black pixels are less intense than red pixels. The area inside the dashed square was taken to obtain the average red spectrum in Fig. 2a.

A scan rate of 100 V·s^{-1} was chosen to prevent any degradation of the molecule while in its oxidized state [33]. It is important to note that we do not interpret the peak to peak separations since electron transfer limitations cannot be easily decorrelated from those due to ohmic drop. Indeed, no ohmic drop compensation procedure was used in order to perform the measurement as soon as possible after rinsing the electrode. This may be performed in a future study.

The recorded voltammograms (Fig. 3) displayed well-resolved peaks with a bell-shape behavior corresponding to the reversible oxidation of the ferrocene entities with apparent standard potentials at +389 ± 10 mV *vs* SCE. The corresponding surface coverages quickly increased during the first 30 min to finally reach Γ = 1.2 × 10^{-6} mol·m^{-2} after 3 h, therefore in qualitative agreement with a rough estimation of the compact packing of the molecules estimated considering hexagonal pavement with a molecular diameter of 0.9 nm (2.3 × 10^{-6} mol·m^{-2}) and in qualitative agreement with our XPS estimations and typical values obtained for other NHCs on gold [62,63]. Longer immersion times occasionally resulted in reproducibility issues regarding surface coverage. This may be due to a competition between adsorption and organization in the monolayer with partial degradation of the layer possibly leading to detachment of the electroactive entity. At the present stage, further investigations are necessary to explain such variations.

Notably, the time necessary for significant surface coverage with MICs is larger than that required with thiols, indicating an activation limited process. While the stability of NHCs coatings on NPs or surfaces is usually addressed by replacement experiments [19,21,26,41,43], we
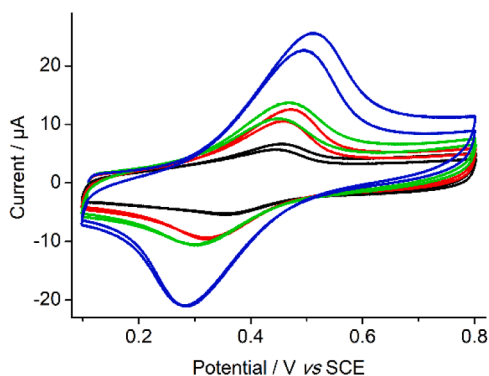
realized that such stability tests may be fruitfully exploited in the fabrication of partial or mixed SAMs. This would pave the way towards alternative strategies for adjusting molecular coverage, and importantly for producing multifunctional surfaces. We thus proceeded to examine the reversibility of thiol incorporation in MIC monolayers or *vice versa*. Using the same protocol developed for **MIC 2**, we coated an electrode with **MIC 1** over 18 h (Γ = 8.3 × 10^{-7} mol·m^{-2}). Following immersion of the electrode into a 1 mM dodecanethiol solution (THF), we observed a gradual decrease of molecular coverage leading to almost complete loss of all redox entities after 3 h as shown in Fig. 4. However, when the same electrode was once again immersed in a solution of **MIC 1** for 3 h, 75 % of the initial **MIC 1** coverage was recovered evidencing effective **MIC 1** incorporation. It is nevertheless very likely that thiols were still present on the electrode surface as suggested by the larger standard potential (528 *vs* 464 mV) most likely resulting from an increased hydrophobic environment near the redox centers [64]. We suggest that in the partial pavement vacancies of the MIC-functionalized electrode surface, there is still room for some smaller dodecanethiol molecules that are then not removed.

These experiments contrast with results from literature for which no exchange was observed [33,36], and deserve further discussion. Thiol interactions with gold have been studied by many experimental and theoretical methods [65,66]. Desorption experiments indicated a bond energy of 127 kJmol^{-1} [67]. As early as 1994, enhanced mobility of gold atoms ligated by thiolates was spotted by Weiss et al., based on STM experiments [68]. Later, single molecule AFM and STM experiments demonstrated that when pulling a dithiol away from the surface, rupture

Fig. 3. Cyclic voltammograms obtained in 0.1 M tetrabutylammonium hexa-fluorophosphate (dichloromethane) for a gold electrode modified with **MIC 2** during 5 (black), 15 (red), 60 (green) and 180 (blue) minutes. Two consecutive cycles were recorded.
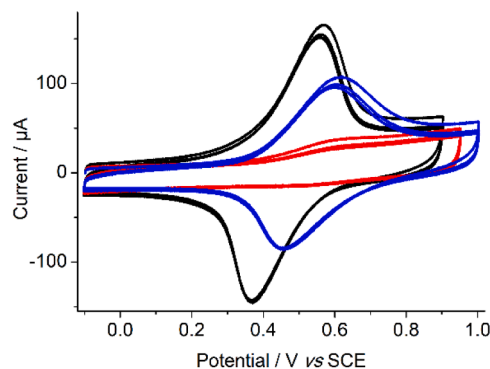

Fig. 4. Initial signal obtained after immersion of a gold electrode in 1 mM **MIC 1** for 18 h (Γ = 8.3 × 10^{-7} mol·m^{-2}, black), then 3 h in 1 mM dodecanethiol (red), then again in 1 mM **MIC 1** for 3 h (Γ = 6.2 × 10^{-7} mol·m^{-2}, blue). Three consecutive cycles.

occurs between two gold atoms and not between Au and S [69–74]. This emphasizes that the metal/ligand bond is not the only parameter to consider.

Returning to carbenes, the bond strength is about 150 kJmol^{-1}, and DFT calculations suggest that coordination on-top of a gold atom is more favorable [33,75]. Here also, Glorius demonstrated that Au-carbene entities are mobile on the surface [29]. We also note that for NHC-capped gold NPs, stability tests show very different results depending on the ligands, solvents and ionic concentrations involved, with only a few systems presenting good resistance to thiol exchange [19,21,26,41,43]. We therefore suggest that initial coverage of the monolayer is also an important parameter, exchange being favored at lower coverages or at monolayers containing more defects. Further-more, to reach the surface, Van der Waals interaction that may favor incorporation of the carbene in the preexisting layer may be favorable. As support of this hypothesis and illustration of the complexity of these replacement experiments, we performed similar experiments with **MIC 2** as shown in Fig. S8. In this case, we could not significantly displace dodecanethiol while both MIC structures (**1** and **2**) are similar and hence probably their Au-C bond strengths.

3. Conclusion

Therefore, this work introduces a novel route, beyond the traditional Au-S affinity, to provide complex and multifunctional SAMs. Impor-tantly, it is also shown that mixed MIC/thiol SAMs with different relative compositions may be created. The ease of preparation of functional MICs in comparison with NHCs will pave the way for future applications. Further studies will aim at understanding and controlling the grafting mechanism and organization, and to extend the methodology to other substrates, such as 2D materials [76].

CRediT authorship contribution statement

Omar Sadek: Writing – original draft, Investigation, Data curation. **Jad Rabah:** Writing – original draft, Investigation, Data curation. **Salem Ba Sowid:** Investigation. **Dimitri Mercier:** Investigation, Data curation. **Philippe Marcus:** Data curation. **Clément Chauvier:** Investigation, Data curation. **François Ribot:** Writing – review & editing, Supervision, Investigation, Funding acquisition, Data curation. **Louis Fensterbank:** Writing – review & editing, Supervision, Project administration, Fund-ing acquisition, Data curation, Conceptualization. **Emmanuel Mai-sonhaute:** Supervision, Funding acquisition, Data curation, Conceptualization.

Declaration of competing interest

The authors declare that they have no known competing financial interests or personal relationships that could have appeared to influence the work reported in this paper.

Data availability

Data will be made available on request.

Acknowledgments

Supplementary materials

Supplementary material associated with this article can be found, in the online version, at doi:10.1016/j.electacta.2024.145189.

References

[1] R.L. Carroll, C.B. Gorman, The genesis of molecular electronics, Angew. Chem., Int. Ed. 41 (2002) 4378–4400, https://doi.org/10.1002/1521-3773(20021202)41:23<4378::AID-ANIE4378>3.0.CO;2-A.

[2] C.D. Bain, E.B. Troughton, Y.T. Tao, J. Evall, G.M. Whitesides, R.G. Nuzzo, Formation of monolayer films by the spontaneous assembly of organic thiols from solution onto gold, J. Am. Chem. Soc. 111 (1989) 321–335, https://doi.org/10.1021/ja00183a049.

[3] S. Cosnier, A. Karyakin, Electropolymerization: Concepts, Materials and Applications, Wiley-VCH, 2010.

[4] D. Bélanger, J. Pinson, Electrografting: a powerful method for surface modification, Chem. Soc. Rev. 40 (2011) 3995–4048, https://doi.org/10.1039/C0CS00149J.

[5] T. Matrab, C. Combellas, F. Kanoufi, Scanning electrochemical microscopy for the direct patterning of a gold surface with organic moities derived from iodonium salt, Electrochem. Commun. 10 (2008) 1230–1234, https://doi.org/10.1016/j.elecom.2008.06.006.

[6] Y.R. Leroux, H. Fei, J.M. Noël, C. Roux, P. Hapiot, Efficient covalent modification of a carbon surface: use of a silyl protecting group to form an active monolayer, J. Am. Chem. Soc. 132 (2010) 14039–14041, https://doi.org/10.1021/ja106971x.

[7] L.T. Nielsen, K.H. Vase, M. Dong, F. Besenbacher, S.U. Pedersen, K. Daasbjerg, Electrochemical approach for constructing a monolayer of thiophenolates from grafted multilayers of diaryl disulfides, J. Am. Chem. Soc. 129 (2007) 1888–1889, https://doi.org/10.1021/ja0682430.

[8] L. Pichereau, L. Fillaud, N. Kostopoulos, E. Maisonhaute, T. Cauchy, M. Allain, J. Noel, C. Gautier, T. Breton, Highly reactive diazenyl radical species evidenced during aryldiazonium electroreduction, J. Phys. Chem. Lett. 13 (2022) 11866–11871, https://doi.org/10.1021/acs.jpclett.2c0308911866.

[9] O. Pluchery, Y. Zhang, R. Benbalagh, L. Caillard, J.J. Gallet, F. Bournel, A.F. Lamic-Humblot, M. Salmeron, Y.J. Chabal, F. Rochet, Static and dynamic electronic characterization of organic monolayers grafted on a silicon surface, Phys. Chem. Chem. Phys. 18 (2016) 3675–3684, https://doi.org/10.1039/C5CP05943G.

[10] A.V. Zhukhovitskiy, M.J. MacLeod, J.A. Johnson, Carbene ligands in surface chemistry: from stabilization of discrete elemental allotropes to modification of nanoscale and bulk substrates, Chem. Rev. 115 (2015) 11503–11532, https://doi.org/10.1021/acs.chemrev.5b00220.

[11] C.A. Smith, M.R. Narouz, P.A. Lummis, I. Singh, A. Nazemi, C.H. Li, C.M. Crudden, N-heterocyclic carbenes in materials chemistry, Chem. Rev. 119 (2019) 4986–5056, https://doi.org/10.1021/acs.chemrev.8b00514.

[12] Y. An, J. Yu, Y. Han, Recent advances in the chemistry of N-heterocyclic-carbene-functionalized metal-nanoparticles and their applications, Chin. J. Chem. 37 (2019) 76–87, https://doi.org/10.1002/cjoc.201800450.

[13] G. Kaur, R.L. Thimes, J.P. Camden, D.M. Jenkins, Fundamentals and applications of N-heterocyclic carbene functionalized gold surfaces and nanoparticles, Chem. Commun. 58 (2022) 13188–13197, https://doi.org/10.1039/D2CC05183D.

[14] M. Koy, P. Bellotti, M. Das, F. Glorius, N-Heterocyclic carbenes as tunable ligands for catalytic metal surfaces, Nat. Catal. 4 (2021) 352–363, https://doi.org/10.1038/s41929-021-00607-z.

[15] E. Hurst, K. Wilson, I. Fairlamb, V. Chechik, N-Heterocyclic carbene coated metal nanoparticles, New J. Chem. 33 (2009) 1837–1840, https://doi.org/10.1039/b905559b.

[16] J. Vignolle, T.D. Tilley, N-Heterocyclic carbene-stabilized gold nanoparticles and their assembly into 3D superlattices, Chem. Commun. (2009) 7230–7232, https://doi.org/10.1039/B913884F.

[17] C. Serpell, J. Cookson, A. Thompson, C. Brown, P. Beer, Haloaurate and halopalladate imidazolium salts: structures, properties, and use as precursors for catalytic metal nanoparticles, Dalton Trans. 42 (2013) 1385–1393, https://doi.org/10.1039/c2dt31984e.

[18] A. Ferry, K. Schaepe, P. Tegeder, C. Richter, K. Chepiga, B. Ravoo, F. Glorius, Negatively charged N-heterocyclic carbene-stabilized Pd and Au nanoparticles and efficient catalysis in water, ACS Catal. 5 (2015) 5414–5420, https://doi.org/10.1021/acscatal.5b01160.

[19] M. MacLeod, J. Johnson, PEGylated N-heterocyclic carbene anchors designed to stabilize gold nanoparticles in biologically relevant media, J. Am. Chem. Soc. 137 (2015) 7974–7977, https://doi.org/10.1021/jacs.5b02452.

[20] M.R. Narouz, C.H. Li, A. Nazemi, C.M. Crudden, Amphiphilic N-heterocyclic carbene-stabilized gold nanoparticles and their self-assembly in polar solvents, Langmuir 33 (2017) 14211–14219, https://doi.org/10.1021/acs.langmuir.7b02248.

[21] K. Salorinne, R. Man, C. Li, M. Taki, M. Nambo, C. Crudden, Water-soluble N-heterocyclic carbene-protected gold nanoparticles: size-controlled synthesis, stability, and optical properties, Angew. Chem., Int. Ed. 56 (2017) 6198–6202, https://doi.org/10.1002/anie.201701605.

[22] N. Nosratabad, Z. Jin, L. Du, M. Thakur, H. Mattoussi, N-heterocyclic carbene-stabilized gold nanoparticles: mono-versus multidentate ligands, Chem. Mater. 33 (2021) 921–933, https://doi.org/10.1021/acs.chemmater.0c03918.

[23] N. Bridonneau, L. Hippolyte, D. Mercier, D. Portehault, M.D.E. Murr, P. Marcus, L. Fensterbank, C. Chanéac, F. Ribot, N-heterocyclic carbene-stabilized gold nanoparticles with tunable sizes, Dalton Trans. 47 (2018) 6850–6859, https://doi.org/10.1039/C8DT00416A.

[24] X. Frogneux, L. Hippolyte, D. Mercier, D. Portehault, C. Chanéac, C. Sanchez, P. Marcus, F. Ribot, L. Fensterbank, S. Carenco, Direct synthesis of N-heterocyclic carbene-stabilized copper nanoparticles from an N-heterocyclic carbene–borane, Chem. A Eur. J. 25 (2019) 11481–11485, https://doi.org/10.1002/chem.201901534.

[25] Q. Wu, R. Peng, F. Gong, Y. Luo, H. Zhang, Q. Cui, Aqueous synthesis of N-heterocyclic carbene-protected gold nanoclusters with intrinsic antibacterial activity, Colloids Surf. A Physicochem. Eng. Asp. 645 (2022) 128934, https://doi.org/10.1016/j.colsurfa.2022.128934.

[26] R.W.Y. Man, C.H. Li, M.W.A. MacLean, O.V. Zenkina, M.T. Zamora, L.N. Saunders, A. Rousina-Webb, M. Nambo, C.M. Crudden, Ultrastable gold nanoparticles modified by bidentate N-heterocyclic carbene ligands, J. Am. Chem. Soc. 140 (2018) 1576–1579, https://doi.org/10.1021/jacs.7b08516.

[27] A. Zhukhovitskiy, M. Mavros, T. Van Voorhis, J. Johnson, Addressable carbene anchors for gold surfaces, J. Am. Chem. Soc. 135 (2013) 7418–7421, https://doi.org/10.1021/ja401965d.

[28] C.M. Crudden, J.H. Horton, M.R. Narouz, Z. Li, C.A. Smith, K. Munro, C.J. Baddeley, C.R. Larrea, B. Drevniok, B. Thanabalasingam, A.B. McLean, O.V. Zenkina, I.I. Ebralidze, Z. She, H.B. Kraatz, N.J. Mosey, L.N. Saunders, A. Yagi, Simple direct formation of self-assembled N-heterocyclic carbene monolayers on gold and their application in biosensing, Nat. Commun. 7 (2016) 12654, https://doi.org/10.1038/ncomms12654.

[29] G. Wang, A. Ruhling, S. Amirjalayer, M. Knor, J. Ernst, C. Richter, H. Gao, A. Timmer, H. Gao, N. Doltsinis, F. Glorius, H. Fuchs, Ballbot-type motion of N-heterocyclic carbenes on gold surfaces, Nat. Chem. 9 (2017) 152–156, https://doi.org/10.1038/NCHEM.2622.

[30] D. Nguyen, M. Freitag, C. Gutheil, K. Sotthewes, B. Tyler, M. Bockmann, M. Das, F. Schluter, N. Doltsinis, H. Arlinghaus, B. Ravoo, F. Glorius, An arylazopyrazole-based N-heterocyclic carbene as a photoswitch on gold surfaces: light-switchable wettability, work function, and conductance, Angew. Chem. Int. Ed. 59 (2020) 13651–13656, https://doi.org/10.1002/anie.202003523.

[31] L. Sherman, S. Strausser, R. Borsari, D. Jenkins, J. Camden, Imidazolinium N-heterocyclic carbene ligands for enhanced stability on gold surfaces, Langmuir 37 (2021) 5864–5871, https://doi.org/10.1021/acs.langmuir.1c00314.

[32] E. Amit, L. Dery, S. Dery, S. Kim, A. Roy, Q. Hu, V. Gutkin, H. Eisenberg, T. Stein, D. Mandler, F. Dean Toste, E. Gross, Electrochemical deposition of N-heterocyclic carbene monolayers on metal surfaces, Nat. Commun. 11 (2020) 5714, https://doi.org/10.1038/s41467-020-19500-7.

[33] C.M. Crudden, J.H. Horton, I.I. Ebralidze, O.V. Zenkina, A.B. McLean, B. Drevniok, Z. She, H.B. Kraatz, N.J. Mosey, T. Seki, E.C. Keske, J.D. Leake, A. Rousina-Webb, G. Wu, Ultra stable self-assembled monolayers of N-heterocyclic carbenes on gold, Nat. Chem. 6 (2014) 409–414, https://doi.org/10.1038/nchem.1891.

[34] A. Bakker, M. Freitag, E. Kolodzieski, P. Bellotti, A. Timmer, J. Ren, B. Lammers, D. Moock, H. Roesky, H. Monig, S. Amirjalayer, H. Fuchs, F. Glorius, An electron-rich cyclic (Alkyl)(Amino)carbene on Au(111), Ag(111), and Cu(111) surfaces, Angew. Chem. Int. Ed. 59 (2020) 13643–13646, https://doi.org/10.1002/anie.201915618.

[35] E.A. Doud, R.L. Starr, G. Kladnik, A. Voevodin, E. Montes, N.P. Arasu, Y. Zang, P. Zahl, A. Morgante, L. Venkataraman, H. Vázquez, D. Cvetko, X. Roy, Cyclopropenylidenes as strong carbene anchoring groups on Au surfaces, J. Am. Chem. Soc 142 (2020) 19902–19906, https://doi.org/10.1021/jacs.0c10743.

[36] D.S. Lee, I. Singh, A.J. Veinot, M.D. Aloisio, J.T. Lomax, P.J. Ragogna, C.M. Crudden, Mesoionic carbene-based self-assembled monolayers on gold, Chem. Sci. 15 (2024) 2480–2485, https://doi.org/10.1039/D3SC04720B.

[37] A. Zhukhovitskiy, M. Mavros, T. Van Voorhis, J. Johnson, Addressable carbene anchors for gold surfaces, J. Am. Chem. Soc. 135 (2013) 7418–7421, https://doi.org/10.1021/ja401965d.

[38] M. Albrecht, Abnormal carbenes as ligands in transition metal chemistry: curiosities with exciting perspectives, Chimia 63 (2009) 105–110, https://doi.org/10.2533/chimia.2009.105.

[39] G. Guisado-Barrios, M. Soleilhavoup, G. Bertrand, 1H-1,2,3-triazol-5-ylidenes: readily available mesoionic carbenes, Acc. Chem. Res. 51 (2018) 3236–3244, https://doi.org/10.1021/acs.accounts.8b00480.

[40] L. Cui, M. Du, S. Guo, Preparation, characterization and stability studies of gold nanoparticles capped by 1,2,3-triazole-based mesoionic carbenes, ChemistrySelect 7 (2022), https://doi.org/10.1002/slct.202201999.

[41] D.T.H. Nguyen, M. Bélanger-Bouliga, L.R. Shultz, A. Maity, T. Jurca, A. Nazemi, Robust water-soluble gold nanoparticles via polymerized mesoionic N-heterocyclic carbene–gold(I) complexes, Chem. Mater. 33 (2021) 9588–9600, https://doi.org/10.1021/acs.chemmater.1c02899.

[42] D. Nguyen, L. Shultz, T. Jurca, A. Nazemi, Monomeric and polymeric mesoionic N-heterocyclic carbene- tethered silver nanoparticles: synthesis, stability, and catalytic activity, Langmuir (2023), https://doi.org/10.1021/acs.langmuir.2c02864.

[43] A. Porcheron, O. Sadek, S. Sowid, N. Bridonneau, L. Hippolyte, D. Mercier, P. Marcus, L. Mutalliev, C. Chauvier, C. Chaneac, L. Fensterbank, F. Ribot, Direct synthesis of mesoionic carbene (MIC)-stabilized gold nanoparticles from 1,2,3-tri-azolium salts, Chem. Mater. 35 (2023) 6865–6876, https://doi.org/10.1021/acs.chemmater.3c01162.

[44] E. Maisonhaute, O. Sadek, J. Rabah, D. Mercier, P. Marcus, C. Chauvier, F. Ribot, L. Fensterbank, Tailored functional monolayers made from mesoionic carbenes, ChemRxiv; Doi:10.26434/Chemrxiv-2023-Dcwqr (2023). https://chemrxiv.org/engage/chemrxiv/article-details/6522f6c7bda59ceb9a215d43.

[45] J.F. DeJesus, M.J. Trujillo, J.P. Camden, D.M. Jenkins, N-heterocyclic carbenes as a robust platform for surface-enhanced Raman spectroscopy, J. Am. Chem. Soc. 140 (2018) 1247–1250, https://doi.org/10.1021/jacs.7b12779.

[46] L.M. Sherman, M.D. Finley, R.K. Borsari, N. Schuster-Little, S.L. Strausser, R.J. Whelan, D.M. Jenkins, J.P. Camden, N-heterocyclic carbene ligand stability on gold nanoparticles in biological media, ACS Omega 7 (2022) 1444–1451, https://doi.org/10.1021/acsomega.1c06168.

[47] R.M. Stöckle, Y.D. Suh, V. Deckert, R. Zenobi, Nanoscale chemical analysis by Tip-Enhanced Raman Spectroscopy, Chem. Phys. Lett. 318 (2000) 131–136, https://doi.org/10.1016/S0009-2614(99)01451-7.

[48] F. Shao, F. Müller, Y. Zhang, A.D. Schlüter, R. Zenobi, Nanoscale chemical imaging of interfacial monolayers by Tip-Enhanced Raman Spectroscopy, Angew. Chem. Int. Ed. 56 (2017) 9361–9366, https://doi.org/10.1002/anie.201703800.

[49] D. Kurouski, A. Dazzi, R. Zenobi, A. Centrone, Infrared and Raman chemical imaging and spectroscopy at the nanoscale, Chem. Soc. Rev. 49 (2020) 3315–3347, https://doi.org/10.1039/C8CS00916C.

[50] X. Wang, S.C. Huang, T.X. Huang, H.S. Su, J.H. Zhong, Z.C. Zeng, M.H. Li, B. Ren, Tip-Enhanced Raman Spectroscopy for surfaces and interfaces, Chem. Soc. Rev. 46 (2017) 4020–4041, https://doi.org/10.1039/C7CS00206H.

[51] T. Touzalin, A.L. Dauphin, S. Joiret, I.T. Lucas, E. Maisonhaute, Tip enhanced Raman spectroscopy imaging of opaque samples in organic liquid, Phys. Chem. Chem. Phys. 18 (2016) 15510–15513, https://doi.org/10.1039/c6cp02596j.

[52] T. Touzalin, S. Joiret, I.T. Lucas, E. Maisonhaute, Electrochemical Tip-Enhanced Raman Spectroscopy imaging with 8 nm lateral resolution, Electrochem. Commun. 108 (2019), https://doi.org/10.1016/j.elecom.2019.106557.

[53] T. Touzalin, S. Joiret, E. Maisonhaute, I.T. Lucas, Capturing electrochemical transformations by Tip-Enhanced Raman Spectroscopy, Curr. Opin. Electrochem. 6 (2017) 46–52, https://doi.org/10.1016/j.coelec.2017.10.016.

[54] J.H.K. Pfisterer, M. Baghernejad, G. Giuzio, K.F. Domke, Reactivity mapping of nanoscale defect chemistry under electrochemical reaction conditions, Nat. Commun. 10 (2019) 5702, https://doi.org/10.1038/s41467-019-13692-3.

[55] N.M. Sabanés, A. Elizabeth, J.H.K. Pfisterer, K.F. Domke, The effect of STM parameters on tip-enhanced Raman spectra, Faraday Discuss. 205 (2017) 233–243, https://doi.org/10.1039/C7FD00164A.

[56] J. Kalbacova, R.D. Rodriguez, V. Desale, M. Schneider, I. Amin, R. Jordan, D.R.T. Zahn, Chemical stability of plasmon-active silver tips for Tip-Enhanced Raman Spectroscopy, Nanospectroscopy 1 (2014) 12–18, https://doi.org/10.2478/nansp-2014-0002.

[57] W. Kim, N. Kim, E. Lee, D. Kim, Z. Hwan Kim, J. Won Park, A tunable Au core–Ag shell nanoparticle tip for tip-enhanced spectroscopy, Analyst 141 (2016) 5066–5070, https://doi.org/10.1039/C6AN00035E.

[58] T. Touzalin, S. Joiret, E. Maisonhaute, I.T. Lucas, Complex electron transfer pathway at a microelectrode captured by *in situ* nanospectroscopy, Anal. Chem. 89 (2017) 8974–8980, https://doi.org/10.1021/acs.analchem.7b01542.

[59] A.J. Bard, L.R. Faulkner, Electrochemical Methods: Fundamentals and Applications, Wiley India Ltd., New Delhi, 2004.

[60] G. Boitel-Aullen, L. Fillaud, F. Huet, I. Nierengarten, B. Delavaux-Nicot, J. Nierengarten, E. Maisonhaute, Electron transfer inside a decaferrocenylated rotaxane analyzed by fast scan cyclic voltammetry and impedance spectroscopy, ChemElectroChem 8 (2021) 3506–3511, https://doi.org/10.1002/celc.202100738.

[61] X.S. Zhou, B.W. Mao, C. Amatore, R.G. Compton, J.L. Marignier, M. Mostafavi, J.F. Nierengarten, E. Maisonhaute, Transient electrochemistry: beyond simply temporal resolution, Chem. Commun. 52 (2016) 251–263, https://doi.org/10.1039/C5CC07953E.

[62] J. Ren, M. Freitag, Y. Gao, P. Bellotti, M. Das, B. Schulze Lammers, H. Mönig, Y. Zhang, C.G. Daniliuc, S. Du, H. Fuchs, F. Glorius, Reversible self-assembly of an N-heterocyclic carbene on metal surfaces, Angew. Chem. Int. Ed. 61 (2022), https://doi.org/10.1002/anie.202115104 e202115104.

[63] H.K. Kim, A.S. Hyla, P. Winget, H. Li, C.M. Wyss, A.J. Jordan, F.A. Larrain, J.P. Sadighi, C. Fuentes-Hernandez, B. Kippelen, J.L. Brédas, S. Barlow, S.R. Marder, Reduction of the work function of gold by N-heterocyclic carbenes, Chem. Mater. 29 (2017) 3403–3411, https://doi.org/10.1021/acs.chemmater.6b04213.

[64] C. Amatore, E. Maisonhaute, B. Schöllhorn, J. Wadhawan, Ultrafast voltammetry for probing interfacial electron transfer in molecular wires, ChemPhysChem 8 (2007) 1321–1329, https://doi.org/10.1002/cphc.200600774.

[65] C. Vericat, M. Vela, G. Benitez, P. Carro, R. Salvarezza, Self-assembled monolayers of thiols and dithiols on gold: new challenges for a well-known system, Chem. Soc. Rev. 39 (2010) 1805–1834, https://doi.org/10.1039/b907301a.

[66] T. Bürgi, Properties of the gold–sulphur interface: from self-assembled monolayers to clusters, Nanoscale 7 (2015) 15553–15567, https://doi.org/10.1039/C5NR03497C.

[67] D.J. Lavrich, S.M. Wetterer, S.L. Bernasek, G. Scoles, Physisorption and chemisorption of alkanethiols and alkyl sulfides on Au(111), J. Phys. Chem. B 102 (1998) 3456–3465, https://doi.org/10.1021/jp980047v.

[68] S.J. Stranick, A.N. Parikh, D.L. Allara, P.S. Weiss, A new mechanism for surface diffusion: motion of a substrate-adsorbate complex, J. Phys. Chem. 98 (1994) 11136–11142, https://doi.org/10.1021/j100094a024.

[69] W. Haiss, S. Martín, E. Leary, H. van Zalinge, S.J. Higgins, L. Bouffier, R.J. Nichols, Impact of junction formation method and surface roughness on single molecule conductance, J. Phys. Chem. C 113 (2009) 5823–5833, https://doi.org/10.1021/jp811142d.

[70] I.V. Pobelov, K.P. Lauritzen, K. Yoshida, A. Jensen, G. Mészáros, K.W. Jacobsen, M. Strange, T. Wandlowski, G.C. Solomon, Dynamic breaking of a single gold bond, Nat. Commun. 8 (2017) 15931, https://doi.org/10.1038/ncomms15931.

[71] K. Yoshida, I.V. Pobelov, D.Z. Manrique, T. Pope, G. Mészáros, M. Gulcur, M.R. Bryce, C.J. Lambert, T. Wandlowski, Correlation of breaking forces, conductances and geometries of molecular junctions, Sci. Rep. 5 (2015) 9002, https://doi.org/10.1038/srep09002.

[72] X. Zhou, L. Liu, P. Fortgang, A. Lefevre, A. Serra-Muns, N. Raouafi, C. Amatore, B. Mao, E. Maisonhaute, B. Schollhorn, Do molecular conductances correlate with electrochemical rate constants? Experimental insights, J. Am. Chem. Soc. 133 (2011) 7509–7516, https://doi.org/10.1021/ja201042h.

[73] U. Rashid, W. Bro-Jorgensen, K. Harilal, P. Sreelakshmi, R. Mondal, V. Pisharam, K. Parida, K. Geetharani, J. Hamill, V. Kaliginedi, Chemistry of the Au-Thiol Interface through the lens of single-molecule flicker noise measurements, J. Am. Chem. Soc. 146 (2024) 9063–9073, https://doi.org/10.1021/jacs.3c14079.

[74] Y. Xue, X. Li, H. Li, W. Zhang, Quantifying thiol–gold interactions towards the efficient strength control, Nat. Commun. 5 (2014) 4348, https://doi.org/10.1038/ncomms5348.

[75] E.A. Doud, M.S. Inkpen, G. Lovat, E. Montes, D.W. Paley, M.L. Steigerwald, H. Vázquez, L. Venkataraman, X. Roy, *In situ* formation of N-heterocyclic carbene-bound single-molecule junctions, J. Am. Chem. Soc 140 (2018) 8944–8949, https://doi.org/10.1021/jacs.8b05184.

[76] L. Li, S. Mahapatra, J.F. Schultz, X. Zhang, N. Jiang, Single-molecule spectroscopic probing of N-heterocyclic carbenes on a two-dimensional metal, Chem (2024), https://doi.org/10.1016/j.chempr.2024.08.013.